Negative Thermal Expansion of Ultrathin Metal Nanowires: A Computational Study

Duc Tam Ho,[†] Soon-Yong Kwon,[‡] Harold S. Park,[§] and Sung Youb Kim[*,†]

[†]Department of Mechanical Engineering, [‡]School of Material Science and Engineering, Ulsan National Institute of Science and Technology, Ulsan 44919, South Korea

[§]Department of Mechanical Engineering, Boston University, Boston, Massachusetts 02215, United States

S *Supporting Information*

ABSTRACT: Most materials expand upon heating because the coefficient of thermal expansion (CTE), the fundamental property of materials characterizing the mechanical response of the materials to heating, is positive. There have been some reports of materials that exhibit negative thermal expansion (NTE), but most of these have been in complex alloys, where NTE originates from the transverse vibrations of the materials. Here, we show using molecular dynamics simulations that some single crystal monatomic FCC metal nanowires can exhibit NTE along the length direction due to a novel thermomechanical coupling. We develop an analytic model for the CTE in nanowires that is a function of the surface stress, elastic modulus, and nanowire size. The model suggests that the CTE of nanowires can be reduced due to elastic softening of the materials and also due to surface stress. For the nanowires, the model predicts that the CTE reduction can lead to NTE if the nanowire Young's modulus is sufficiently reduced while the nanowire surface stress remains sufficiently large, which is in excellent agreement with the molecular dynamics simulation results. Overall, we find a "smaller is smaller" trend for the CTE of nanowires, leading to this unexpected, surface-stress-driven mechanism for NTE in nanoscale materials.

KEYWORDS: *Negative thermal expansion, metal nanowire, surface stress, elastic softening, molecular dynamics*

Positive Thermal Expansion — Bulk Metals — Heating — α_b

Negative Thermal Expansion — Metal Nanowires — D — Heating —
$$\alpha = \alpha_b - \frac{4(1-\nu)}{DE^2}\left(\frac{\partial f}{\partial T}E - \frac{\partial E}{\partial T}f\right)$$
E: Young's modulus; f: surface stress; ν: Poisson's ratio.
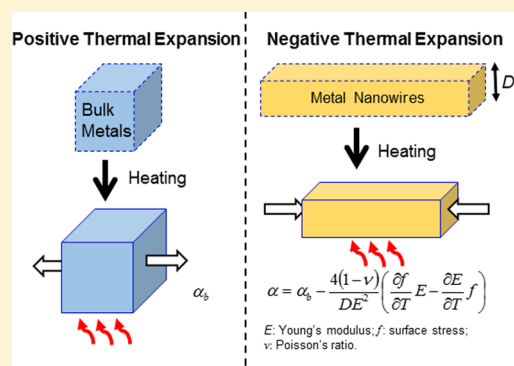
The coefficient of thermal expansion (CTE) α along a particular direction is defined as $\alpha = \frac{1}{L}\frac{\partial L}{\partial T}$ where L and T are the length and temperature, respectively. Most materials have a positive CTE, and thus they expand upon heating, while a much smaller class of materials with negative CTE shrink as the temperature increases. Materials with a negative thermal expansion (NTE) property have various potential applications such as fillers in controlled thermal expansion composites,[1] photoelectric devices,[2] aerospace technology,[3] and as dental materials.[4] The most common mechanism enabling NTE materials is transverse vibrations.[5−7] The key characteristic of these materials is that their crystal structures are essentially networks of corner-linked polyhedrals, which can cause transverse vibration modes, for example, the ZrV_2O_8 family,[8] ZrV_2O_7 family,[9] $Sc_2W_3O_{12}$ family,[10] Cu_2O and Ag_2O,[11] and ReO_3 and ScF_3.[12] In addition, the translation vibration model,[13] phase transformations,[14] and magnetovolume effect[15] are also other mechanisms for NTE, and NTE has recently been observed in architected metamaterials.[16] A few nanoscale materials also exhibit NTE, e.g., graphene[17] and Si nanowires,[18] due to the transverse bending mode, and CuO due to the magnetovolume effect.[19] Au particles with the size of 4 nm show NTE as the temperature is larger than 125 K,[20] and it has been systematically shown later that the NTE is driven by large

electronic excitations.[21] Some experimental studies reported that CTEs of Zn and Cu nanowires were smaller than those of the bulk counterparts (but still positive) due to effect of grain boundaries.[22] Overall, most occurrences of NTE have been in complex alloys, with very few reports in single crystal nanomaterials.

Metal nanowires often show superior physical properties in comparison with their bulk counterparts, including a larger elastic range,[23] higher strength,[24] and smaller thermal conductivity.[25] The key factor governing the unique mechanical behavior and properties of metal nanowires is surface stress. Specifically, due to the surface stress, which is typically tensile in FCC metal nanowires, a compressive stress is induced in the core of the nanowires.[26] The surface stress can cause interesting and unexpected behaviors in nanowires such as phase transformations,[26] shape memory, and pseudoelasticity.[27] Recently, some reports showed that metal nanoplates[28,29] and metal nanowires[30] exhibit negative Poisson's ratio while their bulk counterparts have positive Poisson's ratios partly due to the effect of surface stress. While surface stress effects have been primarily used to explain various mechanical properties of

nanoscale materials, it was rarely been used to explain unique thermal or thermomechanical properties such as NTE.

In this study, we show using molecular dynamics (MD) simulations that some FCC metal [100]-nanowires can show NTE, which is in contrast to the positive CTE observed in the corresponding bulk FCC metal. In addition, we develop an analytic model for CTE in nanowires that is a function of the surface stress, elastic modulus, and nanowire size. While general continuum formulations incorporating surface stress were developed previously,[31,32] the present work is specific to the nanowire geometry, while also focusing on thermomechanical properties (NTE) rather than elastic or purely mechanical properties. Our combined analytic/computational approach shows that the CTE of the nanowires results from a combination of the positive contribution from the expansion between atom pairs and the negative contribution from a thermomechanical coupling connected to surface stress and elastic softening of materials upon heating. Specifically, the tensile surface stresses cause a contraction along the axial direction of the nanowires, leading to a state of compressive stress within the nanowire. Upon heating, the FCC metals soften elastically, and thus the compression increases causing the reduction of CTE. When the surface stress is sufficiently large and the Young's modulus is sufficiently small, the negative contribution becomes significant, and the CTE can turn negative. The prediction of our model is in excellent agreement with MD simulation results. Overall, the present study demonstrates an important effect of surface stress as a critical mechanism governing the thermomechanical properties of nanoscale materials, thus providing a new mechanism for NTE in nanomaterials.

We first present the response upon heating using MD simulations of an Au [100]/{001}nanowire; i.e., the nanowire has a [100]-axial orientation and four {100} side surfaces. The nanowire has a square cross-section and a thickness of 4.3 nm. The four edges of the nanowire were filleted with a radius of 1.0 nm to reduce the likelihood of defect nucleation from the edges at lower temperatures. The interactions between atoms are described by an embedded-atom-method (EAM) potential model.[33] Details of the simulation techniques can be seen in the Simulation Method section. Before discussing the temperature dependence of the lattice parameter, we note that all of the lattice parameters we report in Figure 1 are smaller than the bulk Au lattice parameter of 4.08 Å, which is due to the axial contraction in the nanowires that results from the tensile surface stresses.

As shown in Figure 1, a strong temperature dependence of the lattice parameter along the x-direction a_x is observed. Below 140 K, the nanowire slightly expands along its length as the temperature increases. However, when the temperature exceeds 140 K, we observe a contraction upon heating, and the contraction becomes more significant at higher temperatures. The simulation data of the lattice parameter is fitted to the function $y = aT^3 + bT + c$ where c can be regarded as the lattice parameter of the nanowire at 0 K. The change of the linear CTE α with temperature is then obtained by using the equation:

$$\alpha = \frac{1}{a_x}\frac{\partial a_x}{\partial T} \qquad (1)$$

We also plot in Figure 1 the change of the linear CTE of the Au nanowire with temperature. The linear CTE (purple dash-
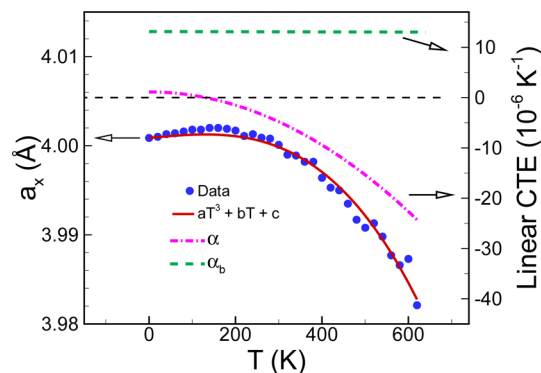
Figure 1. Mechanical response of Au [100] nanowires with the thickness of 4.3 nm on heating. The change of the lattice parameter along the x-direction (a_x) with temperature data is fitted to the function $a_x = F(T) = aT^3 + bT + c$, with $a = -8.774 \times 10^{-11}$, $b = -4.496 \times 10^{-5}$, and $c = 4.001$; the R-square value of the fitting is 0.9817. The nanowire expands as the temperature increases at low temperature range. However, it shrinks upon heating at temperatures higher than the critical temperature of 140 K. As a result, the NTE behavior is observed in the nanowire when the temperature is larger than the critical temperature. On the other hand, the corresponding bulk material shows positive thermal expansion over the entire temperature range.

dot line) is about 1.1×10^{-6} K^{-1} at 0 K and monotonically decreases with temperature and then turns negative at the critical temperature of about 140 K. Clearly, NTE is observed in the nanowire over a large temperature range. The linear CTE of bulk Au in our simulation (green dashed line in Figure 1) is 13×10^{-6} K^{-1} which is close to the experimental value of 14×10^{-6} K^{-1},[34] with the bulk linear CTE being temperature-insensitive. This demonstrates that the thermomechanical properties of Au change significantly at nanometer length scales, with the possibility of NTE. We note that the definition of α in eq 1 is the CTE along the axial direction of the nanowire. The volumetric coefficient of thermal expansion α_V is defined as $\alpha_V = \frac{1}{V}\frac{\partial V}{\partial T}$ where V is the volume of a unit cell of the material. For isotropic and cubic materials, $\alpha_V = 3\alpha$. While linear CTEs of a bulk FCC metal along the principal directions are the same, the linear CTE of the nanowire along the axial direction is not the same as those along the y- and z-directions due to surface stress which will be discussed in detail later. As shown in Figure S1 in the Supporting Information part, the volumetric CTE of the Au [100]-nanowire with the thickness of 4.3 nm is not negative in the temperature range. This indicates that the linear CTEs in the nonaxial directions are not negative. As the result, the nanowire shows NTE along the axial direction whereas the volumetric CTE is positive. This behavior was also observed in other materials in bulk form such as an organic crystalline material[35] and bulk SnSe with the Pnma phase.[36] We now examine the mechanisms enabling the unique property in the metal nanowire.

To further understand the mechanism for the NTE in the Au nanowires, we now focus on the contribution of surface stress. While surface stress can in general be tensile or compressive, the surface stresses associated with (001) surfaces of FCC metals are typically tensile, as shown in previous studies.[37−39] The tensile surface stress causes a contraction along the length direction of the nanowires with an equilibrium compressive strain ε_e with respect to the ideal state of the bulk counterpart.

Then, the relationship between the lattice parameter of the nanowire and that of the bulk material a_b is

$$a_x = a_b(1 + \varepsilon_e) \qquad (2)$$

Substituting eq 2 into eq 1, the linear CTE of the nanowires is given as

$$\alpha = \alpha_b + \frac{1}{1 + \varepsilon_e} \frac{\partial \varepsilon_e}{\partial T} \qquad (3)$$

where $\alpha_b = \frac{1}{a_b} \frac{\partial a_b}{\partial T}$ is the linear CTE of the bulk material.

Although nanowires are overall stress-free at equilibrium for all temperatures, the atoms within the nanowire core are under a multiaxial stress condition due to the surface stress.[30] The corresponding strains can be obtained by using Hooke's law for elastic materials:

$$\boldsymbol{\varepsilon} = \mathbf{S}(\boldsymbol{\varepsilon}): \sigma \qquad (4)$$

where $\mathbf{S}$ is the compliance tensor of the core, which is a function of deformation, i.e., the strain tensor $\boldsymbol{\varepsilon}$. For a square cross section [100]/{001} nanowire with thickness D, the stress components in the core are approximated as (σ_{xx}, σ_{yy}, σ_{zz}, σ_{xy}, σ_{xz}, σ_{yz}) = $(-4f/D, -2f/D, -2f/D, 0, 0, 0)$[30] where f is the surface stress along the [100]-direction on a {001} surface. The strain component of the core in the x-direction is then obtained as

$$\varepsilon_x = \frac{-4f(1 - \nu)}{DE} \qquad (5)$$

where E and ν, which are the Young's modulus along the [100]-direction and Poisson's ratio for [100]-direction stretch and measured for a $\langle 100 \rangle$-direction of the core, respectively. The two elastic properties are calculated from the bulk material as functions of stress. This strain component of the core along the x-direction is also the equilibrium strain of the nanowire. Note that the Young's modulus and Poisson's ratio are functions of deformation.[40] We also note that, in our MD simulations, the Poisson's ratio is almost independent of temperature. Assuming that the Poisson's ratio is temperature-independent, substituting eq 5 into eq 3 gives

$$\alpha = \alpha_b - \frac{4(1 - \nu)}{[DE - 4f(1 - \nu)]E}\left(\frac{\partial f}{\partial T}E - \frac{\partial E}{\partial T}f\right) \qquad (6)$$

In our simulations, DE is two orders larger than $4f(1 - \nu)$, so eq 6 can be further simplified as,

$$\alpha = \alpha_b - \frac{4(1 - \nu)}{DE^2}\left(\frac{\partial f}{\partial T}E - \frac{\partial E}{\partial T}f\right) \qquad (7)$$

The prediction of the nanowire linear CTE in eq 7 requires that the Young's modulus E and surface stress f be determined as functions of temperature. Since there is no explicit expression for these mechanical properties, we directly calculate E and f using MD simulations. Details of the calculation can be seen in the Simulation Method section. Figure 2a plots the simulation data of the Young's modulus of bulk Au along the [100]-direction and the surface stress along the [100]-direction of the Au (001) surface as functions of temperature. The circles and squares indicate the simulation data, while the solid lines are the fitting lines. Clearly, the Young's modulus linearly decreases with temperature. This result is consistent with other simulation results,[41] as well as experimental observations,[42] as
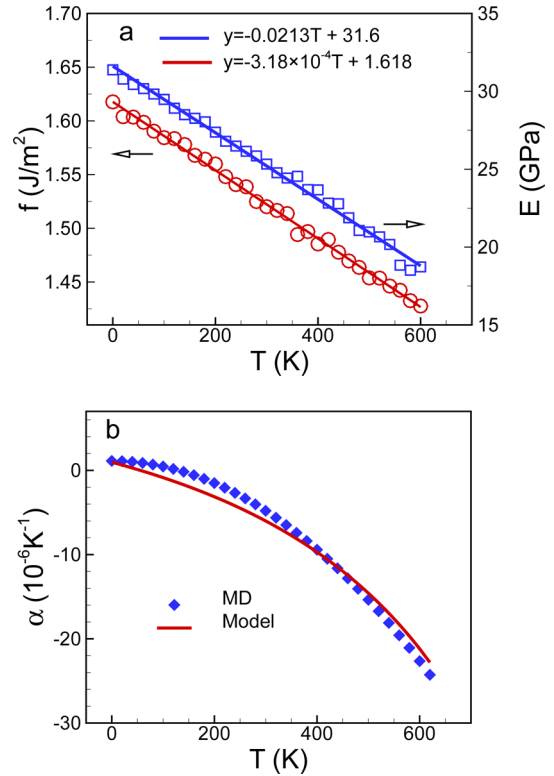
Figure 2. Prediction of the theory and MD simulation results of the linear CTE of the Au [100]-nanowire. a: Change of the surface stress of Au (100) and Young's modulus of Au bulk along the [100]-direction with temperature. b: Prediction by eq 7 versus the MD simulation results. The nanowire has a thickness of 4.3 nm. The prediction by the model is in good agreement with the MD simulation results.

was systematically explained in a previous study.[43] Similarly, the surface stress linearly decreases with temperature.

Equation 7 shows that the nanowire linear CTE α is a combination of the linear CTE of the bulk material and another term which is related to surface stress, elastic modulus, and nanowire size. As presented in Figure 1, the linear CTE of bulk Au is always positive. This positive contribution is consistent with the natural atomic separation that occurs due to any nonzero temperature. In the case of the second term, the contribution can be negative or positive depending on the magnitudes of E and f and their derivatives with respect to temperature. The decrease of the surface stress with temperature $\left(\frac{\partial f}{\partial T} < 0\right)$ causes a positive contribution, whereas the elastic softening $\left(\frac{\partial E}{\partial T} < 0\right)$ causes a negative contribution to the second term. In other words, the reduction of the surface stress tends to enhance, while the elastic softening of the material tends to reduce the linear CTE of the nanowires. As shown in Figure 2a, the decrease in surface stress is 12% over the temperature range, whereas there is a 41% change in the Young's modulus, and thus the elastic softening dominates the contribution to the nanowire linear CTE, leading to an overall reduction in the nanowire linear CTE. In the case of the Au nanowire with the thickness of 4.3 nm, the reduction becomes significant as the temperature increases so that a negative linear CTE is observed when the temperature exceeds 140 K as shown in Figure 1. We note that the linear CTEs along the y- and z-directions of the nanowire are the same, and the

analytical expression can also be obtained by the same procedure for the linear CTE along the axial direction. The linear CTEs along the nonaxial directions are $\beta = \alpha_b - \frac{2(1-3\nu)}{DE^2}\left(\frac{\partial f}{\partial T}E - \frac{\partial E}{\partial T}f\right)$. The sign of the second term of β is different from that of the second term of α because the Poisson's ratio of gold is about 0.44 (>0.33). Consequently, β is positive, whereas α is negative, and thus, the volumetric CTE of the nanowire is positive as presented above.

In the case of ⟨110⟩/{111} Au nanowires, that is, the nanowire has a ⟨110⟩ axial orientation, four {111} side surfaces, and a rhombic cross section, elastic softening does not dominate as in the case of the [100]/{001} nanowire, and thus the linear CTE is almost the same as the bulk counterpart (Figure S2 in the Supporting Information). It is worth mentioning that the Young's modulus of Au in the [110]-direction is about three times larger than in the [100]-direction. This large Young's modulus, which minimizes the surface stress effect, will be discussed in more detail in a later with respect to the NTE trends in other FCC metals. We present in Figure 2b a comparison between the model in eq 7 and the MD simulations of the Au [100]/{001} nanowire with the thickness of 4.3 nm. As can be seen, the prediction of the model is in excellent agreement with the MD simulation results. To underline the generality of our finding, we repeated the MD simulations to calculate the linear CTE of an Au nanowire using another EAM potential.[44] It is shown in Figure S3 in the Supporting Information that the two results are in excellent agreement.

We note that eq 7 implies that the reduction of the linear CTE is inversely proportional to the thickness resulting in a "smaller is smaller" trend. Therefore, the linear CTE of a nanowire can be controlled by simply changing the nanowire size. We confirm this size dependence in Figures S4 and S5 in the Supporting Information. For the case of Au nanowires, the linear CTE is close to zero, and NTE is no longer observed in the considered temperature range when the thickness is larger than 5 nm. For the case of Pt nanowires, the critical thickness for NTE is about 12 nm. These sizes are well-within the reach of current nanowire synthesis techniques, as approaches exist to synthesize sub-2 nm diameter metal nanowires, as shown by Huo and co-workers,[45] and thus, it should be possible to experimentally observe NTE in metal nanowires.

We also note that edges can have significant effects for very small cross section nanowires. As shown in Figure S6, the linear CTE of the nanowires with four edges is more negative than that of nanowires where the edges are filleted. However, the critical temperature for nucleation of dislocation with sharp edges is lower than those with filleted edges because the activation energy for dislocation nucleation initiating from an edge is approximately six times larger than that of side surfaces.[46]

Similar to the edge effect, the effect of cross-sectional shape on the linear CTE of the nanowires is also significant. We plot in Figure S7 the change of the linear CTEs of nanowires with different cross-section shapes. The circular nanowire and the square nanowire have the same thickness of 4.3 nm. The rectangular nanowire has a cross sectional aspect ratio of 2, while having the same cross sectional area as the square nanowire. As can be seen in Figure S7, the linear CTE of the square and rectangular nanowires are nearly the same. However, the linear CTE of the circular nanowire is more negative than the others, especially at high temperature.

We further investigated linear CTEs of various metals. MD simulations were conducted to measure linear CTEs for both bulk and nanowires of the following six metals: Ag, Ni, Cu, Au, Pd, and Pt with the EAM potential developed by Foiles et al.[33] The linear CTEs of the bulk material along the [100]-direction were calculated. They are all positive and nearly temperature-independent over the temperature range as in the case of bulk Au. As shown in Table 1, our MD simulation results are in

Table 1. Comparison of Linear CTE, Young's Modulus, and Surface Stress of Some FCC Metals at an Unstrained State at 0 K

metal	α_b (K^{-1} × 10^{-6})	α_b (K^{-1} × 10^{-6}) [ref 34]	E (GPa)	f (J/m^2)
Ag	21.4	19.5	49	0.81
Ni	15.7	13.0	99	1.29
Cu	17.2	16.6	54	1.37
Au	13.1	14.2	31	1.62
Pd	11.2	11.8	43	2.03
Pt	8.3	9.0	38	2.76

good agreement with those obtained by experiments.[34] The [100]/{001} nanowires are assumed to have the same thickness of $10a_0$ where a_0 is the lattice parameter of the corresponding metals. We show in Figure 3a the change of the linear CTEs of the nanowires with temperature. The linear CTEs are all smaller than the bulk counterparts, which indicates that the softening still plays an important role in the value of the thermomechanical property. However, elastic softening represents a necessary, but not sufficient, condition for the NTE. For
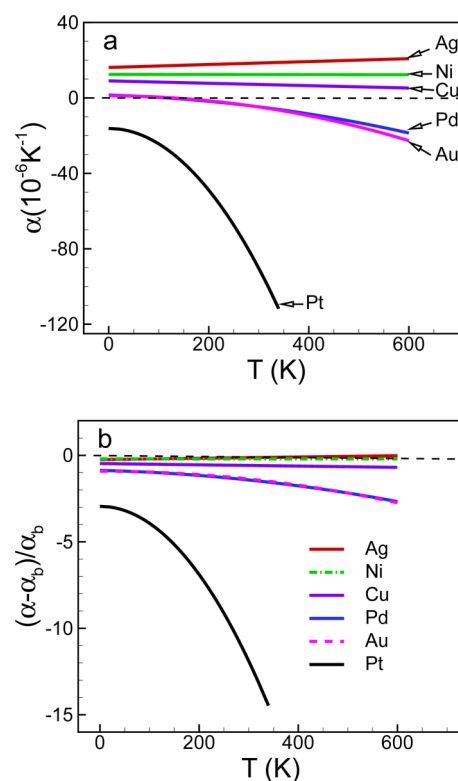
Figure 3. Linear CTEs of various FCC metal [100]-nanowires. a: Xhange of linear CTEs with temperature; b: Xhange of the dimensionless linear CTEs with temperature. For all metals, the nanowires have the same size of $10a_0$. The linear CTE of each nanowire is smaller than that of the bulk counterpart.

NTE, the surface stress should be sufficiently large and the Young's modulus should be sufficiently small. As shown in Figure 3a, the Pt, Pd, and Au nanowires exhibit NTE behavior, whereas Cu, Ni, and Ag nanowires do not. As also shown in Figure 3b, the degree of NTE over the temperature range decreases with the following order: Pt, Pd, Au, Cu, Ni, and Ag, with Pt having the largest NTE. The surface stresses of the six metals are also in the same order.[29] On the other hand, the Young's moduli decrease with the order: Ni, Cu, Ag, Pd, Pt, and Au, whose order is inverted relative to the degree of NTE shown in the previous sentence. This again confirms that while Young's modulus tends to positively contribute, surface stress negatively contributes to the linear CTE of the metal nanowires as expected in eq 7. We also note that, though the Poisson's ratio of the considered metals are all about 0.44, eq 7 also implies that materials with smaller Poisson's ratio will reduce the linear CTE of the nanowire. Recently, it was shown that negative Poisson's ratio constituents can considerably reduce the effective CTE of laminates[47] and hybrid materials.[48]

In conclusion, we have studied the linear CTE of FCC metal [001] nanowires using MD simulations and developed a simple surface stress-based theory for the size and material-dependent linear CTE of FCC metal nanowires. More importantly, we have shown that NTE behavior can be observed in some metal nanowires, while the bulk counterparts all exhibit a positive thermal expansion. In general, the linear CTE of a nanowire is a combination of the linear CTE of the bulk counterpart and a reduction related to surface stress, Young's modulus, and nanowire thickness. Specifically, a linear CTE reduction in nanowires is controlled by surface stress, and a temperature-dependent elastic softening. The linear CTE reduction can become significant and lead to a NTE if the surface stress is sufficiently large and the Young's modulus is sufficiently small. The prediction by the model is in excellent agreement with the MD simulation results. In addition, the linear CTE reduction of [100]/{001} nanowires also increases with decreasing nanowire thickness and thus shows a "smaller is smaller" trend. This study thus elucidates surface stress as a new, nanoscale mechanism for obtaining materials with NTE materials.

Simulation Method. All MD simulations of six FCC (Ag, Au, Cu, Ni, Pd, and Pt) [100]-nanowires and the bulk counterparts are performed by using LAMMPS.[49] The interaction between the atoms is described by the EAM potential model.[33,44] For simplicity of notation, we designate the [100]-, [010]-, and [001]-directions to be the x-, y-, and z-directions, respectively. To model bulk material, we apply periodic boundary conditions along all directions, and the simulation box size is $10a_0 \times 10a_0 \times 10a_0$ where a_0 is the lattice parameter of the material. To model infinite nanowires, we applied periodic boundary conditions along the x-direction, whereas free surface conditions are assigned along the y- and z-directions. In this study, except the case of investigating of edge effect, all edges of the square and rectangular nanowires are filleted with a radius of 1.0 nm to reduce the edge effect, to prevent defect nucleation at higher temperatures. Before applying heat, the nanowires are fully equilibrated at 0 K by using molecular statics simulation. We then increase the temperature from 0 to 20 K by using Langevin dynamics over 100 ps and then anneal the nanowires at 20 K for 200 ps using NPT ensemble to ensure the stress-free condition for the nanowires at 20 K. The simulation data at 20 K is obtained by averaging the data of the last 100 ps of the annealing period. We then repeat the applying temperature step as well as the

annealing step to obtain the response of the structures at 40 K and so on. The simulations for bulk materials are the same as those for the nanowires except that pressure along all directions is maintained to be zero during NPT ensembles.

To obtain the Young's modulus at a given temperature, we start at the well-equilibrated state at that temperature. Then, quasi-MD simulations are employed to get the stress−strain relation. In the quasi-MD simulation, a strain with the value of −0.001 is applied along the x-direction while the pressures along the y- and z-directions are kept zero under the NPT ensemble in 100 ps. Then, after stating at the strain of −0.001, we repeat the simulation with another compressive strain increment of 0.001 until the strain of the bulk material is the same as the strain of the nanowire at the temperature T. To obtain the surface stress f at temperature T, we considered (001) nanoplates with the thickness of $10a_0$. The simulation procedure is the same as that of the nanowire mentioned above. The only difference is that the both stresses along the in-plane directions, i.e., x- and y-directions, are kept zero at each considered temperature instead of only x-stress component which is controlled to be zero in the simulations of the nanowire. At each equilibrium state at a temperature, surface stress is calculated by following a previously described method.[39] This approach, like most others, calculates the surface stress via consideration of an infinite nanoplate such that edge effects are not present. We have discussed above how the nanowire edges in our study were filleted, which reduces the influence of the edge effects on the linear CTE of nanowires, as discussed in the main text as well as in the Supporting Information.

■ ASSOCIATED CONTENT

ⓢ Supporting Information

The Supporting Information is available free of charge on the ACS Publications website at DOI: 10.1021/acs.nano-lett.7b02468.

> Volumetric CTE, simulation results with different potential models, effects of direction, size, edge, and shape on the linear CTE of the metal nanowires (PDF)

■ AUTHOR INFORMATION

Corresponding Author

*E-mail: sykim@unist.ac.kr.

ORCID ⓘ

Duc Tam Ho: 0000-0002-7101-4931

Sung Youb Kim: 0000-0002-9417-4575

Notes

The authors declare no competing financial interest.

■ ACKNOWLEDGMENTS

■ REFERENCES

(1) Lind, C. *Materials* **2012**, *5* (6), 1125−1154.

(2) Cheng, Y.; Liang, Y.; Mao, Y.; Ge, X.; Yuan, B.; Guo, J.; chao, M.; Liang, E. *Mater. Res. Bull.* **2017**, *85*, 176−180.

(3) Imanaka, N.; Hiraiwa, M.; Adachi, G.; Dabkowska, H.; Dabkowski, A. *J. Cryst. Growth* **2000**, *220* (1−2), 176−179.

(4) Grima, J. N.; Zammit, V.; Ruben, G. *Xjenza* **2006**, *11*, 17.

(5) Mary, T. A.; Evans, J. S. O.; Vogt, T.; Sleight, A. W. *Science* **1996**, *272* (5258), 90−92.

(6) Kuzkin, V. A.; Krivtsov, A. M. *Phys. Status Solidi B* **2015**, *252* (7), 1664−1670.

(7) Dove, M. T.; Fang, H. *Rep. Prog. Phys.* **2016**, *79* (6), 066503.

(8) Ernst, G.; Broholm, C.; Kowach, G. R.; Ramirez, A. P. *Nature* **1998**, *396* (6707), 147−149.

(9) Mittal, R.; Chaplot, S. L. *Phys. Rev. B: Condens. Matter Mater. Phys.* **2008**, *78* (17), 174303.

(10) Forster, P. M.; Yokochi, A.; Sleight, A. W. *J. Solid State Chem.* **1998**, *140* (1), 157−158.

(11) Mittal, R.; Chaplot, S. L.; Mishra, S. K.; Bose, P. P. *Phys. Rev. B: Condens. Matter Mater. Phys.* **2007**, *75* (17), 174303.

(12) Liu, Y.; Wang, Z.; Wu, M.; Sun, Q.; Chao, M.; Jia, Y. *Comput. Mater. Sci.* **2015**, *107*, 157−162.

(13) Lakes, R.; Wojciechowski, K. W. *Phys. Status Solidi B* **2008**, *245* (3), 545−551.

(14) Tyagi, A. K.; Achary, S. N.; Mathews, M. D. *J. Alloys Compd.* **2002**, *339* (1−2), 207−210.

(15) Wang, J. L.; Campbell, S. J.; Tegus, O.; Marquina, C.; Ibarra, M. R. *Phys. Rev. B: Condens. Matter Mater. Phys.* **2007**, *75* (17), 174423.

(16) Wang, Q.; Jackson, J. A.; Ge, Q.; Hopkins, J. B.; Spadaccini, C. M.; Fang, N. X. *Phys. Rev. Lett.* **2016**, *117* (17), 175901.

(17) Bao, W.; Miao, F.; Chen, Z.; Zhang, H.; Jang, W.; Dames, C.; Lau, C. N. *Nat. Nanotechnol.* **2009**, *4* (9), 562−566.

(18) Jiang, J.-W.; Wang, J.-S.; Li, B. *Nanoscale* **2010**, *2* (12), 2864−2867.

(19) Zheng, X. G.; Kubozono, H.; Yamada, H.; Kato, K.; Ishiwata, Y.; Xu, C. N. *Nat. Nanotechnol.* **2008**, *3* (12), 724−726.

(20) Li, W.-H.; Wu, S. Y.; Yang, C. C.; Lai, S. K.; Lee, K. C.; Huang, H. L.; Yang, H. D. *Phys. Rev. Lett.* **2002**, *89* (13), 135504.

(21) Comaschi, T.; Balerna, A.; Mobilio, S. *Phys. Rev. B: Condens. Matter Mater. Phys.* **2008**, *77* (7), 075432.

(22) Wang, Y.; Yang, J.; Ye, C.; Fang, X.; Zhang, L. *Nanotechnology* **2004**, *15* (11), 1437.

(23) Yue, Y.; Liu, P.; Zhang, Z.; Han, X.; Ma, E. *Nano Lett.* **2011**, *11* (8), 3151−3155.

(24) Wang, J.; Sansoz, F.; Huang, J.; Liu, Y.; Sun, S.; Zhang, Z.; Mao, S. X. *Nat. Commun.* **2013**, *4*, 1742.

(25) Cheng, Z.; Liu, L.; Xu, S.; Lu, M.; Wang, X. *Sci. Rep.* **2015**, *5*, 10718.

(26) Diao, J.; Gall, K.; Dunn, M. L. *Nat. Mater.* **2003**, *2* (10), 656−660.

(27) Park, H. S.; Gall, K.; Zimmerman, J. A. *Phys. Rev. Lett.* **2005**, *95* (25), 255504.

(28) Ho, D. T.; Park, S.-D.; Kwon, S.-Y.; Park, K.; Kim, S. Y. *Nat. Commun.* **2014**, *5*, 3255.

(29) Ho, D. T.; Kim, H.; Kwon, S.-Y.; Kim, S. Y. *Phys. Status Solidi B* **2015**, *252* (7), 1492−1501.

(30) Ho, D. T.; Kwon, S.-Y.; Kim, S. Y. *Sci. Rep.* **2016**, *6*, 27560.

(31) Gurtin, M. E.; Murdoch, A. I. *Arch. Ration. Mech. Anal.* **1975**, *57* (4), 291−323.

(32) Cammarata, R. C. *Prog. Surf. Sci.* **1994**, *46* (1), 1−38.

(33) Foiles, S. M.; Baskes, M. I.; Daw, M. S. *Phys. Rev. B: Condens. Matter Mater. Phys.* **1986**, *33* (12), 7983−7991.

(34) Coefficients of Linear Thermal Expansion. http://www.engineeringtoolbox.com/linear-expansion-coefficients-d_95.html (accessed Nov 23, 2016).

(35) Das, D.; Jacobs, T.; Barbour, L. J. *Nat. Mater.* **2010**, *9* (1), 36−39.

(36) Liu, G.; Zhou, J.; Wang, H. *Phys. Chem. Chem. Phys.* **2017**, *19*, 15187.

(37) Shenoy, V. B. *Phys. Rev. B: Condens. Matter Mater. Phys.* **2005**, *71* (9), 094104.

(38) Dingreville, R.; Qu, J. *Acta Mater.* **2007**, *55* (1), 141−147.

(39) Ho, D. T.; Park, S.-D.; Lee, H.; Kwon, S.-Y.; Kim, S. Y. *EPL Europhys. Lett.* **2014**, *106* (3), 36001.

(40) Liang, H.; Upmanyu, M.; Huang, H. *Phys. Rev. B: Condens. Matter Mater. Phys.* **2005**, *71* (24), 241403.

(41) Cao, A.; Ma, E. *Acta Mater.* **2008**, *56* (17), 4816−4828.

(42) Chang, Y. A.; Himmel, L. *J. Appl. Phys.* **1966**, *37* (9), 3567−3572.

(43) Pham, H. H.; Williams, M. E.; Mahaffey, P.; Radovic, M.; Arroyave, R.; Cagin, T. *Phys. Rev. B: Condens. Matter Mater. Phys.* **2011**, *84* (6), 064101.

(44) Voter, A. F.; Chen, S. P. *Characterization of Defects in Materials*; Mater. Res. Soc. Symp. Proc. No. 82; Materials Research Society: Pittsburgh, 1987; p 175.

(45) Huo, Z.; Tsung, C.; Huang, W.; Zhang, X.; Yang, P. *Nano Lett.* **2008**, *8* (7), 2041−2044.

(46) Zhu, T.; Li, J.; Samanta, A.; Leach, A.; Gall, K. *Phys. Rev. Lett.* **2008**, *100* (2), 025502.

(47) Lim, T.-C. *Phys. Status Solidi B* **2011**, *248* (1), 140−147.

(48) Pasternak, E.; Shufrin, I.; Dyskin, A. V. *Compos. Struct.* **2016**, *138*, 313−321.

(49) Plimpton, S. *J. Comput. Phys.* **1995**, *117* (1), 1−19.